

1-7987533



Energy, Mines and
Resources Canada

Energie, Mines et
Ressources Canada

CANMET

Canada Centre
for Mineral
and Energy
Technology

Centre canadien
de la technologie
des minéraux
et de l'énergie

CONVERSION FACTORS FOR CALCULATING WORKING LEVELS USING CONTINUOUS
RADON PROGENY TIME-INTEGRATING MONITORS

J. BIGU

ELLIOT LAKE LABORATORY

MARCH 1987

To be submitted for publication in Radiation Protection Dosimetry.

CROWN COPYRIGHTS RESERVED

MINING RESEARCH LABORATORIES
DIVISION REPORT MRL 87-60 (J)



MRL 87-60(J)C.2

MRL 87-60(J)C.2

Canmet Information
Centre

D'information de Canmet

JAN 25 1997

555, rue Booth ST.
Ottawa, Ontario K1A 0G1

CONVERSION FACTORS FOR CALCULATING WORKING LEVELS USING CONTINUOUS
RADON PROGENY TIME-INTEGRATING MONITORS

by

J. Bigu*

ABSTRACT

A theoretical analysis has been carried out of the growth of integrated radon progeny and thoron progeny activity deposited on the sampling filter of continuous, time-integrating, Working Level Monitors. With available microprocessor technology it is shown that the results of this analysis can be used to convert α -particle count rate into Working Level as a function of sampling time from the beginning of the sampling period. This feature is not commonly available in commercial instrumentation which, therefore, do not provide true measurements of the Working Level until a radioactive steady-state in the sampling filter has been attained. This steady-state condition occurs after about 3 h of sampling for the radon progeny and about 15 h for the thoron progeny.

Key words: Radon progeny; Thoron progeny; Working Level monitors.

*Research Scientist and Radiation/Respirable Dust/Ventilation Project Leader, Elliot Lake Laboratory, CANMET, Energy, Mines and Resources Canada, Elliot Lake, Ontario.

INTRODUCTION

There is at present a wide variety of instrumentation available for routine determination of radon progeny in dwellings, uranium mines, uranium mills, and other work locations.

Radon progeny monitors of the continuous, time-integrating, type have become very popular recently. One of the advantages is their conceptual simplicity. Time-integrating, continuous, monitors for radon progeny are usually of the active kind, i.e., they use a pump to sample air. Basically, their operation is as follows. Air is sampled through an 'absolute' filter facing a suitable α -particle detector. Alpha-particle counts registered by the detector and associated electronic circuitry are stored in a memory unit and displayed on command or automatically by means of a digital read-out, after the α -count is internally converted to a suitable radiation level unit, such as Working Level (WL).

Time-integrating radon progeny monitors also have disadvantages, namely, they fail to respond quickly enough to fast changes in radiation level and they do not provide true readings until radioactive steady-state conditions in the sampling filter have been reached. In addition, because of the half-life of the radioisotopes involved, a time-lag between actual radiation level and reported radiation level by the instrument is observed.

The above are factors which significantly limit the practical applicability of time-integrating monitors. The fact that no reliable measurements of the radiation level are available from most instruments before radioactive equilibrium conditions in the filter have been reached constitutes a serious drawback, particularly when environmental monitoring for relatively short periods such as a regular working shift is necessary. Taking into consideration that a normal working shift is reduced to about 6 h for monitoring purposes, and that radioactive steady-state conditions in the

filter are not fully reached before 3 h of sampling for the radon progeny (and much longer for the thoron progeny), the useful monitoring period is reduced to 3 h, a clearly insufficient period for reliable measurements in dynamic field conditions.

This paper provides theoretical and experimental data that enable measurements of radon progeny and thoron progeny to be carried out before as well as after radioactive equilibrium conditions in the sampling filter have been attained. To be of practical value, the data presented would require the use of microprocessor technology.

THEORETICAL BACKGROUND

The rate of growth of activity in the sampling filter of a radiation instrument of the time-integrating, active kind, is given by the following expression:

$$\frac{dA_m}{dt} = C_m Q + \lambda_m A_{m-1} - \lambda_m A_m; \quad (1)$$

where,

A_m and A_{m-1} are the activities of the m -th and $(m-1)$ -th members of the radioactive decay chain on the filter, Bq (pCi), respectively;

C_m is the atmospheric concentration of the m -th member of the radioactive decay chain, Bq m^{-3} (pCi L^{-1});

λ_m is the decay constant of the m -th member of the radioactive decay chain, s^{-1} (min^{-1});

Q is the dosimeter sampling rate, $m^3 s^{-1}$ ($L min^{-1}$).

In the above Equation the simplifying assumption has been made that C_m and Q remain constant during the sampling period. The case where C_m varies in a predictable time-dependent fashion has been investigated elsewhere⁽¹⁾.

The activities on the filter at time T_S after the beginning of sampling are obtained by integrating Equation 1 for each radionuclide of interest. The resulting expressions are denoted by $A_i(T_S)$, $A_j(T_S)$, and $A_k(T_S)$ where the subindices i , j , and k are used to denote, respectively, ^{218}Po or ^{216}Po , ^{214}Pb or ^{212}Pb , and ^{214}Bi or ^{212}Bi . Expressions for these variables have been derived by several authors⁽²⁻⁷⁾. They are given elsewhere⁽⁸⁾ for the benefit of the interested reader in a form suitable for computer coding.

The total activities accumulated in the filter during a sampling time T_{S1} to T_{S2} ($T_{S2} > T_{S1}$) are obtained by integrating the Equations for $A_i(T_S)$, and so on⁽⁸⁾. Calling these integrated activities IA_iS , IA_jS , and IA_kS , where I stands for integrated and S for sampling, it is not difficult to show that:

$$IA_iS = \int_{T_{S1}}^{T_{S2}} A_i(T_S) dT_S = C_i Q \tau_i F_i \quad (2)$$

$$IA_jS = \int_{T_{S1}}^{T_{S2}} A_j(T_S) dT_S = Q \left[C_j \tau_j F_j + C_i \left(\frac{\tau_i^2 F_i}{\tau_i - \tau_j} + \frac{\tau_i \tau_j F_j}{\tau_j - \tau_i} \right) \right] \quad (3)$$

$$IA_kS = \int_{T_{S1}}^{T_{S2}} A_k(T_S) dT_S = Q \left[C_k \tau_k F_k + C_j \left(\frac{\tau_j^2 F_j}{\tau_j - \tau_k} + \frac{\tau_j \tau_k F_k}{\tau_k - \tau_j} \right) + C_i \left(\frac{\tau_i^3 F_i}{(\tau_i - \tau_j)(\tau_i - \tau_k)} + \frac{\tau_i \tau_j^2 F_j}{(\tau_j - \tau_i)(\tau_j - \tau_k)} + \frac{\tau_i \tau_k^2 F_k}{(\tau_k - \tau_i)(\tau_k - \tau_j)} \right) \right] \quad (4)$$

where, $\tau_i = 1/\lambda_i$, $\tau_j = 1/\lambda_j$, and $\tau_k = 1/\lambda_k$.

$$F_i = (T_{S2} - T_{S1}) + \tau_i (e^{-T_{S2}/\tau_i} - e^{-T_{S1}/\tau_i}) \quad (5)$$

$$F_j = (T_{S2} - T_{S1}) + \tau_j (e^{-T_{S2}/\tau_j} - e^{-T_{S1}/\tau_j}) \quad (6)$$

$$F_k = (T_{S2} - T_{S1}) + \tau_k (e^{-T_{S2}/\tau_k} - e^{-T_{S1}/\tau_k}) \quad (7)$$

The total α -activity deposited on the filter during the sampling time $T_{S2} - T_{S1} = \Delta T$ is given by adding Equations 2 and 4.

If the sampling filter of the instrument faces a suitable α -particle detector, as is usually the case, it follows that the number of α -counts, N_α , registered by the α -particle detector and associated electronic circuitry, if any, can be written as follows:

$$N_\alpha = \epsilon \eta \delta (IA_i S + IA_k S) \quad (8)$$

where $IA_i S$ and $IA_k S$ are given in Bq. The symbol δ ($\ll 1$) is inserted to take into account plate-out of α -particles in the instrument sampling head. η ($\ll 1$) represents the fraction of α -particles emerging from the filter. The symbol ϵ is used to denote the α -particle counting efficiency of the detector and its associated electronic circuitry.

The radon progeny activity, $A(\text{Rn})$, corresponding to a total α -count, N_α , measured on the filter is given, from Equation 8, by:

$$A(\text{Rn}) = N_\alpha / \epsilon \Delta T \quad (9)$$

where, $A(\text{Rn})$ is given in Bq and ΔT in s. (The radon progeny α -counting rate, in say, counts per minute, $\text{cpm}(\text{Rn})$, corresponding to ΔT is $\text{cpm}(\text{Rn}) = 60 N_\alpha / \Delta T$.)

The general expression for the Working Level, WL, for radon daughters or thoron daughters is given as:

$$WL = \sum_m WL_m = \left(\frac{2.22}{1.3 \times 10^5} \right) \sum_m C_m \tau_m E_m(\alpha) \quad (10)$$

$E_m(\alpha)$ is the ultimate α -particle energy (MeV) per decaying atom of m -type. The Working Level is defined as the release of 1.3×10^5 MeV of α -particle energy, per litre of air, from the decay of any mixture of ^{218}Po , ^{214}Pb , and ^{214}Bi (radon progeny) or ^{212}Pb and ^{212}Bi (thoron progeny).

The following relationship can be written:

$$A(\text{Rn}) / WL(\text{Rn}) = C_F(\text{Rn}) \quad (11)$$

However, an alternative expression of more practical use in experimental measurements can be written in terms of $\text{cpm}(\text{Rn})$, as follows:

$$\text{cpm}(\text{Rn})/\text{WL}(\text{Rn}) = C_F^{\sim}(\text{Rn}).$$

Since $\text{WL}(\text{Rn})$ is constant if C_m is constant, Equation 11 indicates that $A(\text{Rn})$ or $\text{cpm}(\text{Rn})$ are time-dependent (see Equations 2, 3 and 4). However, it can be shown⁽⁸⁾ that for $T_S \gg \lambda_m^{-1}$, $A(\text{Rn})$ and $\text{cpm}(\text{Rn})$ reach, and remain at, a constant value provided C_m and Q remain constant. Hence, $C_F(\text{Rn})$ attains a constant value if the above conditions are met. For the radon progeny, the above is true for $T_S \gtrsim 240$ min, and nearly true for $T_S \gtrsim 180$ min. The former condition will be referred to as the steady-state condition.

Equation 11 for $T_S > 180$ min is normally used in automated environmental monitors and some personal dosimeters to derive $\text{WL}(\text{Rn})$ from $\text{cpm}(\text{Rn})$ measurements. However, for $T_S \lesssim 180$ min, the instruments give erroneous readings which are disregarded for the reasons discussed above. This is not important for long-term radiation monitoring, but is important for daily working shift sampling as the time during which the instrument does not produce correct data is almost half of the regular working shift. However, with available technology it is not difficult to correct this anomaly.

An expression similar to Equation 11 for the thoron progeny can also be written:

$$A(\text{Tn})/\text{WL}(\text{Tn}) = C_F(\text{Tn}) \quad (12)$$

For the thoron progeny, the time at which steady-state conditions are attained is significantly longer than that corresponding to the radon progeny, as will be shown below. (An alternative, more useful expression for practical purposes can be written: $\text{cpm}(\text{Tn})/\text{WL}(\text{Tn}) = C_F^{\sim}(\text{Tn}).$)

A case of great practical interest is the presence of radon/thoron mixtures found in varying proportions in some uranium mines and other locations. In this case, as the instrument does not discriminate radon progeny α -particles from thoron progeny α -particles, the α -count, recorded by

the instrument corresponds to the total α -count, i .e., $\text{cpm}(\text{total}) = \text{cpm}(\text{Rn}) + \text{cpm}(\text{Tn})$. $\text{WL}(\text{Rn})$ and $\text{WL}(\text{Tn})$ can still be calculated provided the ratio $\text{WL}(\text{Tn})/\text{WL}(\text{Rn}) = \text{WLR}$ is known as indicated below and elsewhere⁽⁹⁾. (It should be noted that some instruments, using α -spectrometry, can differentiate radon progeny from thoron progeny, but their success in providing accurate measurements of both has been rather limited.)

THEORETICAL RESULTS

Figures 1 to 4 show the conversion factors $C_F(\text{Rn})$ and $C_F(\text{Tn})$ versus time calculated according to Equations 11 and 12, respectively. The y-axis scale factors, 60×10^{-3} in Figures 1 to 3 and 60 in Figure 4, can be used to calculate the conversion factors $C_F(\text{Rn})$ and $C_F(\text{Tn})$. However, if the numerical coefficient, 60, is omitted, the alternative factors $\hat{C}_F(\text{Rn})$ and $\hat{C}_F(\text{Tn})$, of more direct practical application, can easily be estimated. It should be noted that the symbol C_F in the above Figures is used to indicate both C_F and \hat{C}_F according to the scale factor used.

Calculation of $C_F(\text{Rn})$ and $C_F(\text{Tn})$ has been done for several radon progeny and thoron progeny concentration ratios, i.e., $X = [^{214}\text{Pb}]/[^{218}\text{Po}]$ and $Y = [^{214}\text{Bi}]/[^{218}\text{Po}]$ for the radon progeny, indicated in the graphs by X:Y, and $K = [^{212}\text{Bi}]/[^{212}\text{Pb}]$, for the thoron progeny. Square brackets are used here to indicate activity concentration.

The values of $C_F(\text{Rn})$ and $C_F(\text{Tn})$ have been normalized to $Q=1 \text{ L min}^{-1}$ and $\epsilon=1$, assuming no α -particle self-absorption in the sampling filter and no radon (thoron) progeny plate-out in the sampling head of the instrument. For values of Q , ϵ , η and δ other than those indicated above, Equations 8, 9, 11 and 12 should be corrected correspondingly. Since the above variables appear as simple multipliers in the Equations of interest, correction of $C_F(\text{Rn})$ and $C_F(\text{Tn})$ for a new set of variables, Q , ϵ , η and δ , is straightforward.

The calculations shown in Figures 1 to 4 have been carried out for sampling intervals $T_{S2}-T_{S1} = 10$ min, and the corresponding values for $C_F(Rn)$ and $C_F(Tn)$ have been plotted as those corresponding to T_{S2} . Because of the short sampling interval, the latter approximation is very nearly accurate.

It should be noted that as $C_F(Rn)$ and $C_F(Tn)$ are representative of $A(Rn)$ or $cpm(Rn)$, and $A(Tn)$ or $cpm(Tn)$, respectively (see Equations 11 and 12), Figures 1 to 4 also indicate, apart from the constant multiplier $WL(Rn)$ or $WL(Tn)$, the integrated α -particle count in a 10 min interval calculated according to Equations 8 and 9.

Figure 1 shows that $C_F(Rn)$ varies rapidly during the first 60 min or so and then progressively more slowly between 60 min and 180 min until a constant value is reached for times greater than about 240 min. A more detailed graph of $C_F(Rn)$ during the first 70 min is shown in Figure 2. Figures 1 and 2 show $C_F(Rn)$ versus time for several radon progeny 'disequilibrium' concentration ratios, indicated as X:Y.

Figure 3 shows that $C_F(Tn)$ varies with time although less rapidly than $C_F(Rn)$. This is so because of the presence of ^{212}Pb , a relatively long-lived radioisotope of 10.6 h half-life, that 'controls' the rate of decay of the short-lived thoron progeny radioactive chain. Figure 4 shows $C_F(Tn)$ during the first 100 min. Figures 3 and 4 have been obtained for several thoron 'disequilibrium' concentration ratios, indicated by K. Figure 3 indicates that steady-state or radioactive equilibrium in the sampling filter is only reached after about 900 min as opposed to approximately 180 min for the case of the radon progeny.

Figures 1 to 4 also show that $C_F(Rn)$ and $C_F(Tn)$ depend on the disequilibrium ratios X, Y and K. Tables 1 and 2 show the calculated values of $C_F(Rn)$ and $C_F(Tn)$ at different sampling intervals for several values of the disequilibrium ratios. Also shown in the Tables are the values

corresponding to $C_F(\text{Rn})$ and $C_F(\text{Tn})$. The data in these Tables indicate that X, Y and K affect $C_F(\text{Rn})$ and $C_F(\text{Tn})$ mostly at low sampling times, i.e., under 60 min for the radon progeny and under about 400 min for the thoron progeny. Furthermore, the effect of K on $C_F(\text{Tn})$ is significantly more pronounced than the effect of X and Y on $C_F(\text{Rn})$.

DISCUSSION OF THEORETICAL RESULTS AND PRACTICAL APPLICATIONS

The data presented above indicate that $C_F(\text{Rn})$ and $C_F(\text{Tn})$ depend on both the elapsed sampling time, and the relationship between the concentration of the short-lived decay products of radon and thoron. The data also suggest that $WL(\text{Rn})$ and $WL(\text{Tn})$ can be calculated from theoretical values of $C_F(\text{Rn})$ and $C_F(\text{Tn})$, respectively, and experimental data for Q, ϵ , η and δ .

It should be noted that while the dependence of C_F on the sampling time does not pose any particular problem, its dependence on the variables X, Y and K often introduces significant uncertainties in the calculation of WL. This is so because X, Y and K are only known by direct experimental measurement. Furthermore, these variables are highly dependent on air flow conditions, which at certain working places, such as underground uranium mines, vary significantly during a working shift. Hence, X, Y and K are expected to change quite frequently. Because of this, and because of the practical difficulties and inconvenience associated with the measurement of X, Y and K, values for C_F can only be assigned based on average field conditions. It should be noted, however, that the uncertainty of C_F decreases with increasing sampling times, as Figures 1 to 4 and Tables 1 and 2 indicate.

The data discussed above are useful for determining WL by monitors that do not provide true values of this variable during the filter

radioactive ingrowth period, i.e., prior to reaching 'steady-state' radioactive conditions. This includes continuous radon progeny Working Level Monitors of the time-integrating type.

However, with presently available microprocessor technology, it is quite straightforward to store C_F values in a memory unit, to keep track of the sampling time after turning the sampling system of the monitor on, and to make the sampling interval, i.e., $T_{S2}-T_{S1}$, programmable. By doing this and writing a simple program, the instrument can identify the 'right', stored, C_F value for any given sampling time and sampling interval, correct the α -particle count and convert the corrected α -count to the true Working Level.

Figure 5 shows some theoretical and experimental radon progeny data for a laboratory instrument prototype in which the above technique was incorporated. The uncorrected values are those assuming a C_F independent of time, i.e., the C_F corresponding to steady-state conditions in the sampling filter. The corrected values are those corresponding to the true C_F , i.e., its time-dependent value. The theoretical data corresponds to the cpm calculated taking into account the operating conditions of the instrument, i.e., $Q=0.2 \text{ L min}^{-1}$ and $\epsilon=0.2$, assuming no plate-out or self-absorption. The difference between theoretical and experimental values is due to plate-out in the sampling head and some α -particle absorption in the filter. The measurements were conducted in a Radon/Thoron Test Facility (RTTF) of the walk-in type.

Under actual field conditions, in say, uranium mines, and mills, X, Y and K are not constant, but representative average values for these variables should be chosen for calculating the Working Level.

The method outlined above is straightforward for the case of radon progeny atmospheres only, or thoron progeny atmospheres only. However, for

an arbitrary mixture of both, a common occurrence in Ontario (Canada) underground uranium mines, the situation is more complicated, but it can be resolved as indicated elsewhere⁽⁹⁾. In this case, the ratio $WL(Tn)/WL(Rn)$ must be known by direct experiment or by choosing representative values corresponding to long-term average field conditions. With present microprocessor technology, however, it is a simple matter to extend the theory outlined here to any mixture of radon progeny and thoron progeny to suit particular field conditions⁽⁹⁾. This would only add a minimum of analytical complexity and time expenditure to the particular cases discussed in this paper.

With present microprocessor technology it is also possible to determine $WL(Tn)/WL(Rn)$ by the instrument from experimental cpm data after the sampling period. This is possible by using a modified version of the Ogden method^(10,11) as indicated elsewhere⁽⁸⁾. Knowledge of the above ratio permits calculation of $WL(Rn)$ and/or $WL(Tn)$ in a manner described elsewhere⁽⁹⁾.

CONCLUSION

With available technology, determination of Working Levels by time-integrating continuous monitors for radon and thoron progeny can be estimated during the period in which the sampling filter of the instrument is in the 'radioactive in-growth period', i.e., before steady-state conditions in the sampling filter have been attained. This is of practical interest because commercially available continuous monitors of the time-integrating kind normally incorporate in their software values for C_F under steady-state conditions only. The in-growth period, even for the radon progeny, is a significant fraction of a regular working shift.

REFERENCES

1. Bigu, J. Theoretical Considerations Regarding Active Sampling of Time-Dependent Radon (Thoron) Atmospheres. Division Report MPR/MRL 85-75(TR) CANMET, Energy, Mines and Resources Canada (1985).
2. Martz, D.E., Holleman, D.F., McCurdy, D.E. and Schiager, K.J. Analysis of atmospheric concentrations of RaA, RaB and RaC by alpha-spectroscopy. Health Phys. 17, 131-138 (1969).
3. Tsivoglou, E.C., Ayer, H.E. and Holaday, D.A. Occurrence of non-equilibrium atmospheric mixtures of radon and its daughters. Nucleonics 11, 40-45 (1953).
4. Thomas, J.W. and LeClare, P.C. A study of the two filter method. Health Phys., 18, 113-122 (1970).
5. Groer, P., Evans, R.D. and Schroeder, G.L. Activity build-up and decay on a filter. Report MIT952-5, Part 1, p 330; Mass. Inst. of Technol. (1968).
6. Evans, R.D. Engineer's guide to the elementary behaviour of radon daughters. Health Phys. 17, 229-252 (1969).
7. Raabe, O.G. and Wrenn, M.E. Analysis of the activity of radon daughter samples by weighted least squares. Health Phys. 17, 593-605 (1969).
8. Bigu, J., Determination of the Working Level of radon/thoron mixtures by personal α -dosimeters and environmental α -monitors using gross α -counting. Int. J. Environ. Monit. Assess. 3, 77-103 (1983).
9. Bigu, J. Theory, operation and performance of a time-integrating, continuous radon (thoron) daughter Working Level monitor. Radiation Prot. Dosimetry 9, 19-26 (1984).
10. Ogden, T.L. A method for measuring the Working Level values of mixed radon and thoron daughters in coal mine air. Ann. Occup. Hyg. 17, 23-34 (1974).

11. Ogden, T.L. Radon and thoron Working Levels from ordinary industrial-hygiene dust samples. Ann. Occup. Hyg. 20, 49-53 (1977).

Table 1 - Calculation of $C_F(Rn)$ for several times and disequilibrium ratios¹

Sampling Interval ($T_{S2}-T_{S1}$) min	X:Y	$C_F(Rn)$	$\hat{C}_F(Rn)$	$\frac{C_F(Rn)_{\min}}{C_F(Rn)_{\max}}$	PD* %
10-20	1.0:1.0	71.69	4301.27	0.765	23
	0.8:0.4	64.61	3876.89		
	0.6:0.3	69.36	4161.38		
	0.4:0.2	77.56	4653.81		
	0.3:0.15	84.41	5065.11		
40-50	1.0:1.0	164.50	9870.14	0.923	7.7
	0.8:0.4	152.47	9148.04		
	0.6:0.3	155.52	9331.50		
	0.4:0.2	160.82	9649.02		
	0.3:0.15	165.24	9914.24		
60-70	1.0:1.0	206.42	12385.08	0.951	4.9
	0.8:0.4	196.88	11812.58		
	0.6:0.3	199.29	11957.43		
	0.4:0.2	203.47	12208.14		
	0.3:0.15	206.96	12417.55		
450-460	1.0:1.0	286.56	17193.81	0.972	2.8
	0.8:0.4	288.45	17306.95		
	0.6:0.3	289.97	17398.19		
	0.4:0.2	292.60	17556.12		
	0.3:0.15	294.80	17688.03		

* PD stands for percentage difference between the max. and min. values of $C_F(Rn)$.

¹ Values have been normalized for $\epsilon=1$ and $Q=1 \text{ L min}^{-1}$.

Table 2 - Calculation of $C_F(Tn)$ for several times and disequilibrium ratios*

Sampling Interval ($T_{S2}-T_{S1}$) min	K	$C_F(Tn)$	$\hat{C}_F(Tn)$	$\frac{C_F(Tn)_{min}}{C_F(Tn)_{max}}$
10-20	1.0	4.15	248.76	0.38
	0.7	3.09	185.19	
	0.5	2.35	140.89	
	0.3	1.58	94.94	
50-60	1.0	15.12	907.53	0.51
	0.7	12.06	723.36	
	0.5	9.92	594.99	
	0.3	7.70	461.88	
90-100	1.0	25.89	1553.59	0.60
	0.7	21.65	1299.21	
	0.5	18.70	1121.93	
	0.3	15.63	938.08	
500-510	1.0	116.22	6973.44	0.91
	0.7	111.91	6714.68	
	0.5	108.91	6534.34	
	0.3	105.79	6347.31	
850-860	1.0	167.63	10057.69	0.96
	0.7	164.67	9880.13	
	0.5	162.61	9756.37	
	0.3	160.47	9628.04	

*Values have been normalized, i.e., $\epsilon=1$, $Q=1$ L min⁻¹.

LIST OF ILLUSTRATIONS

- Figure 1 - Radon progeny conversion factor $CF(Rn)$ versus sampling time for two different disequilibrium ratios. The y-axis scale factor 60×10^{-3} can be used to calculate the conversion factor \hat{C}_F (Bq WL^{-1}). If the numerical coefficient 60 is omitted, the conversion factor C_F (cpm WL^{-1}) can be obtained (see Tables 1 and 2).
- Figure 2 - Radon progeny conversion factor $CF(Rn)$ versus sampling time for several disequilibrium ratios (X:Y). The y-axis scale factor 60×10^{-3} can be used to calculate the conversion factor \hat{C}_F (Bq WL^{-1}). If the numerical coefficient 60 is omitted, the conversion factor C_F (cpm WL^{-1}) can be obtained (see Tables 1 and 2).
- Figure 3 - Thoron progeny conversion factor $CF(Tn)$ versus sampling time for different disequilibrium ratios (K). The y-axis scale factor 60×10^{-3} can be used to calculate the conversion factor \hat{C}_F (Bq WL^{-1}). If the numerical coefficient 60 is omitted, the conversion factor C_F (cpm WL^{-1}) can be obtained (see Tables 1 and 2).
- Figure 4 - Thoron progeny conversion factor $CF(Tn)$ versus sampling time for several disequilibrium ratios (K). The y-axis scale factor 60 can be used to calculate the conversion factor \hat{C}_F (Bq WL^{-1}). If the numerical coefficient is omitted, the conversion factor C_F (cpm WL^{-1}) can be obtained (see Tables 1 and 2).
- Figure 5 - Theoretical, experimental, and corrected α -particle count rate versus sampling time.

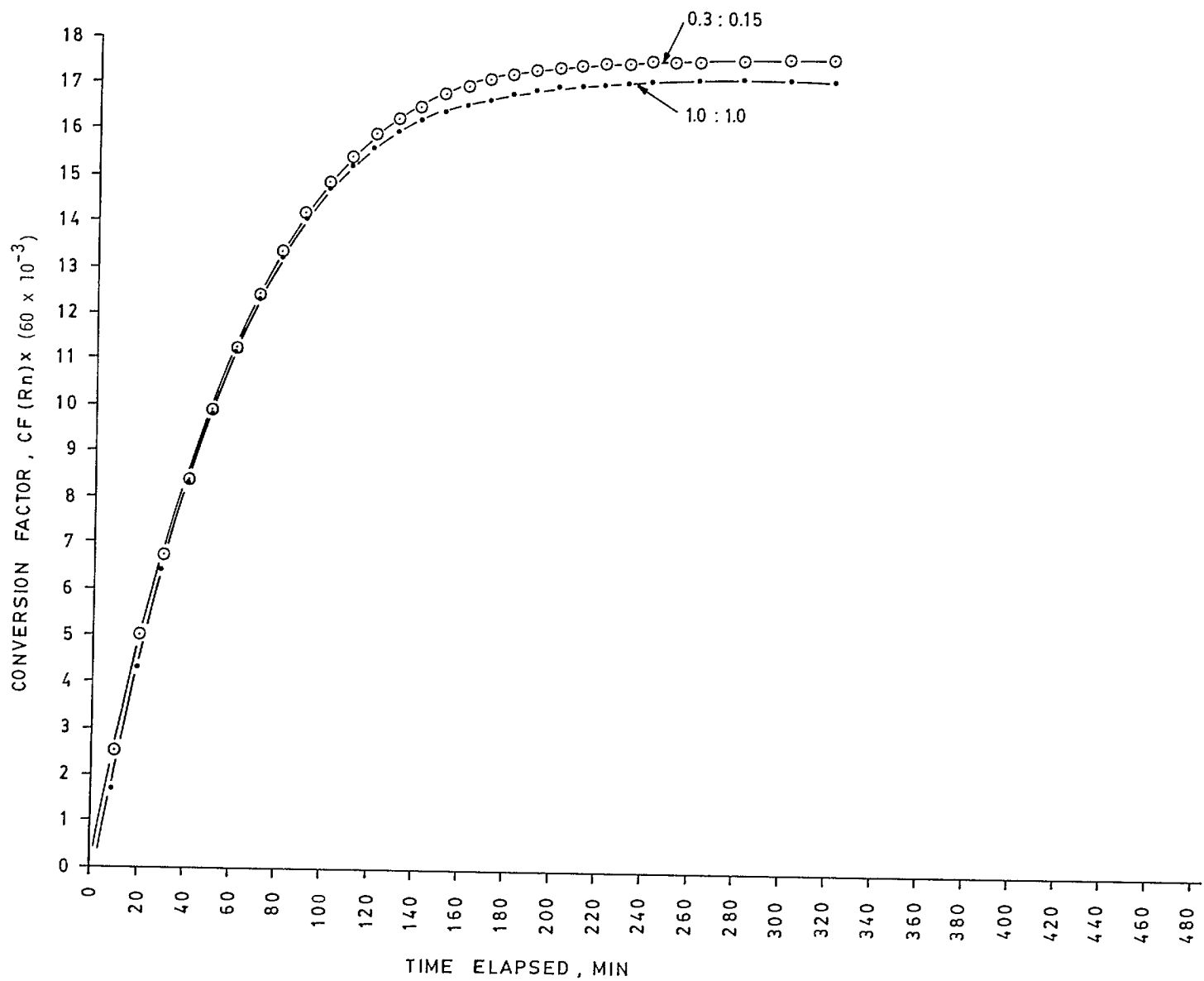


Figure 1 .

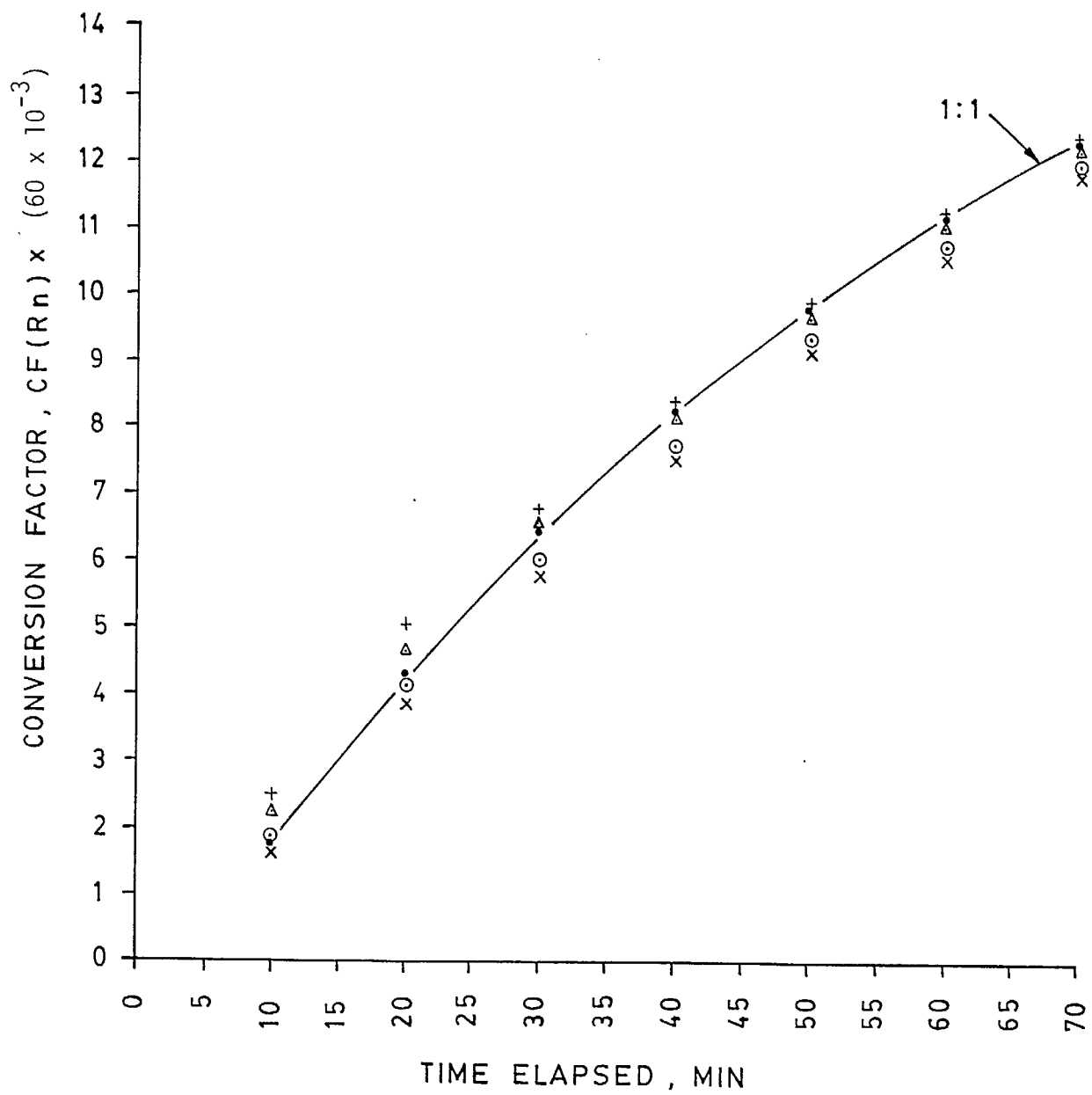


Figure 2

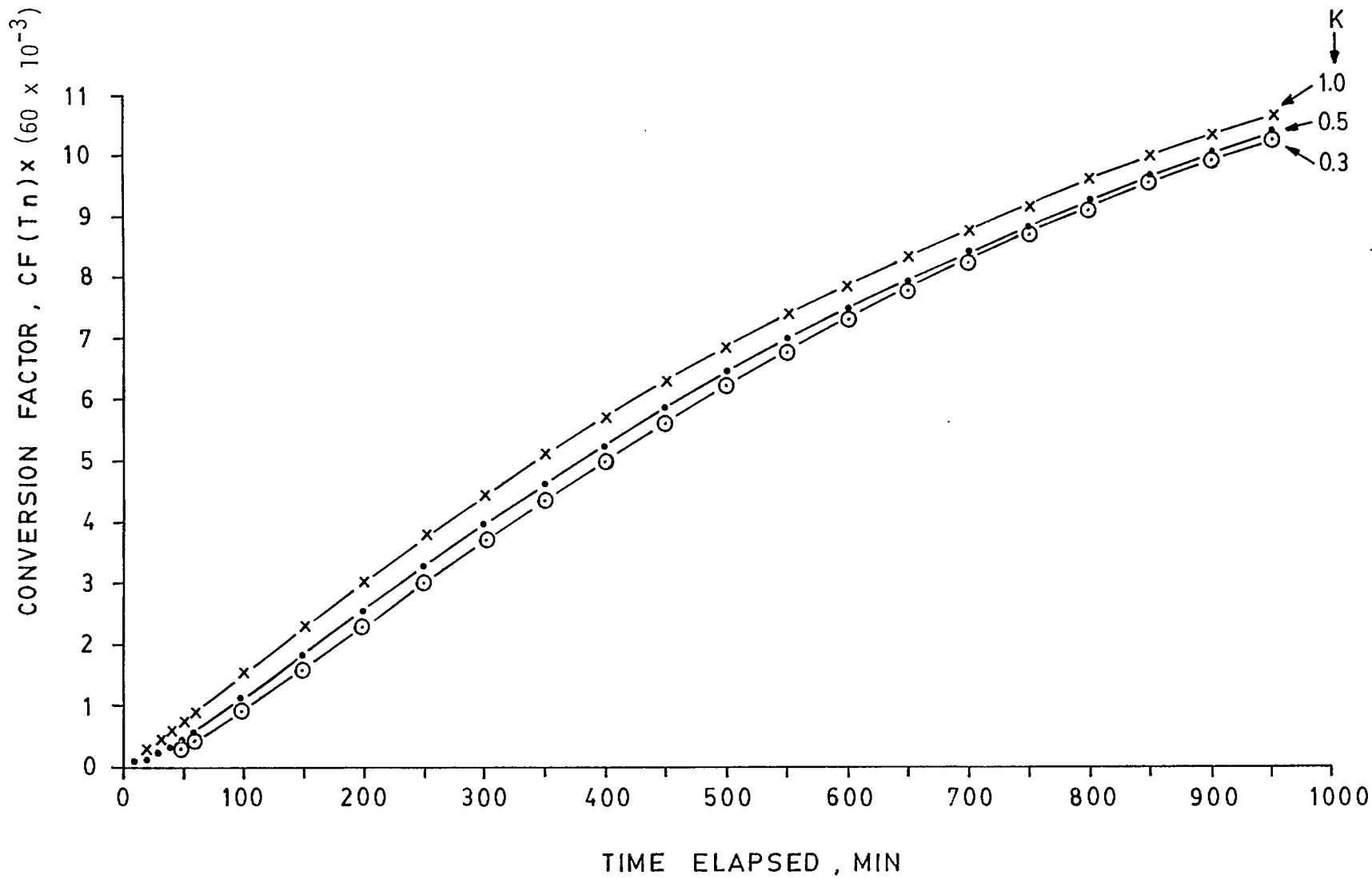


Figure 3

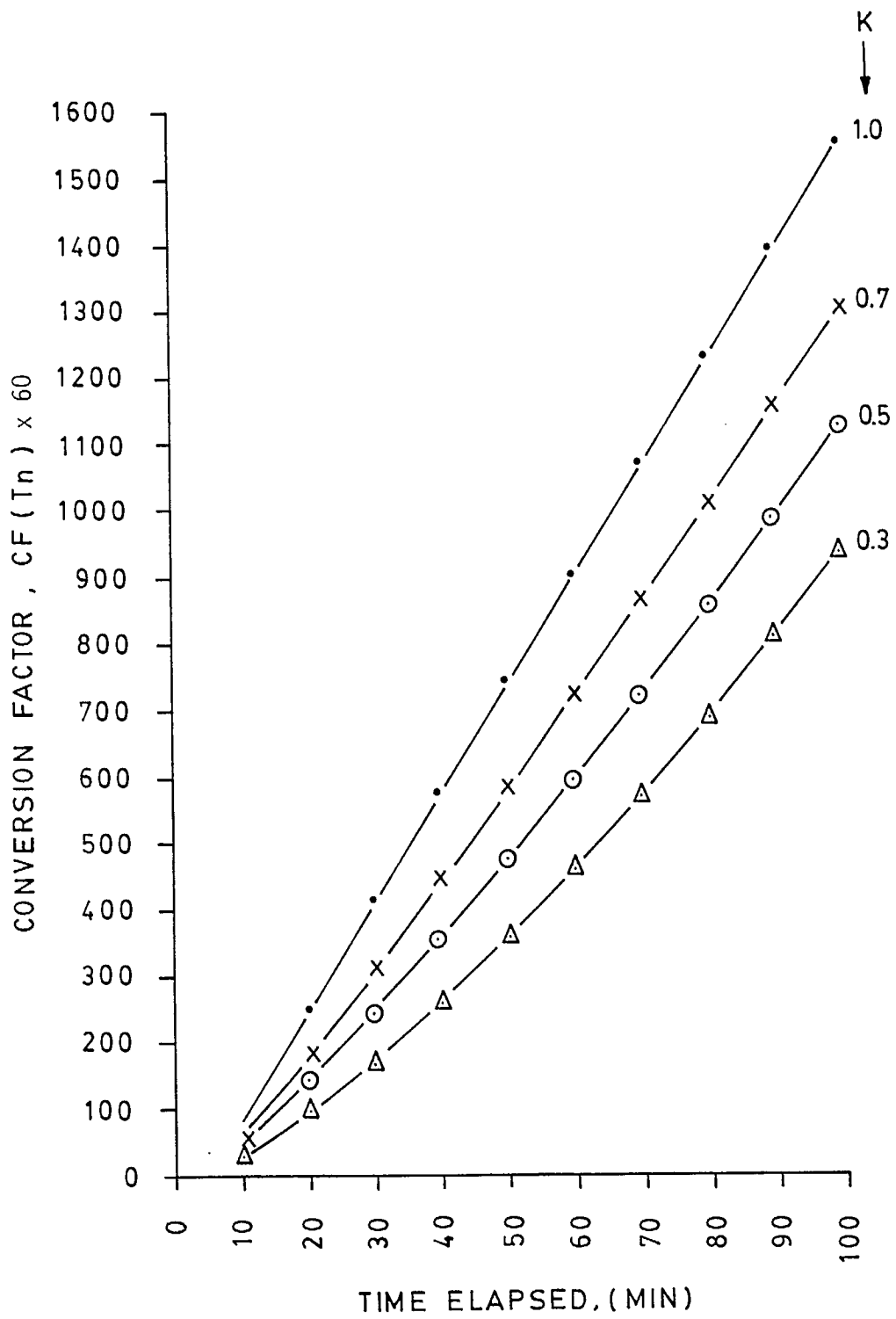


Figure 4

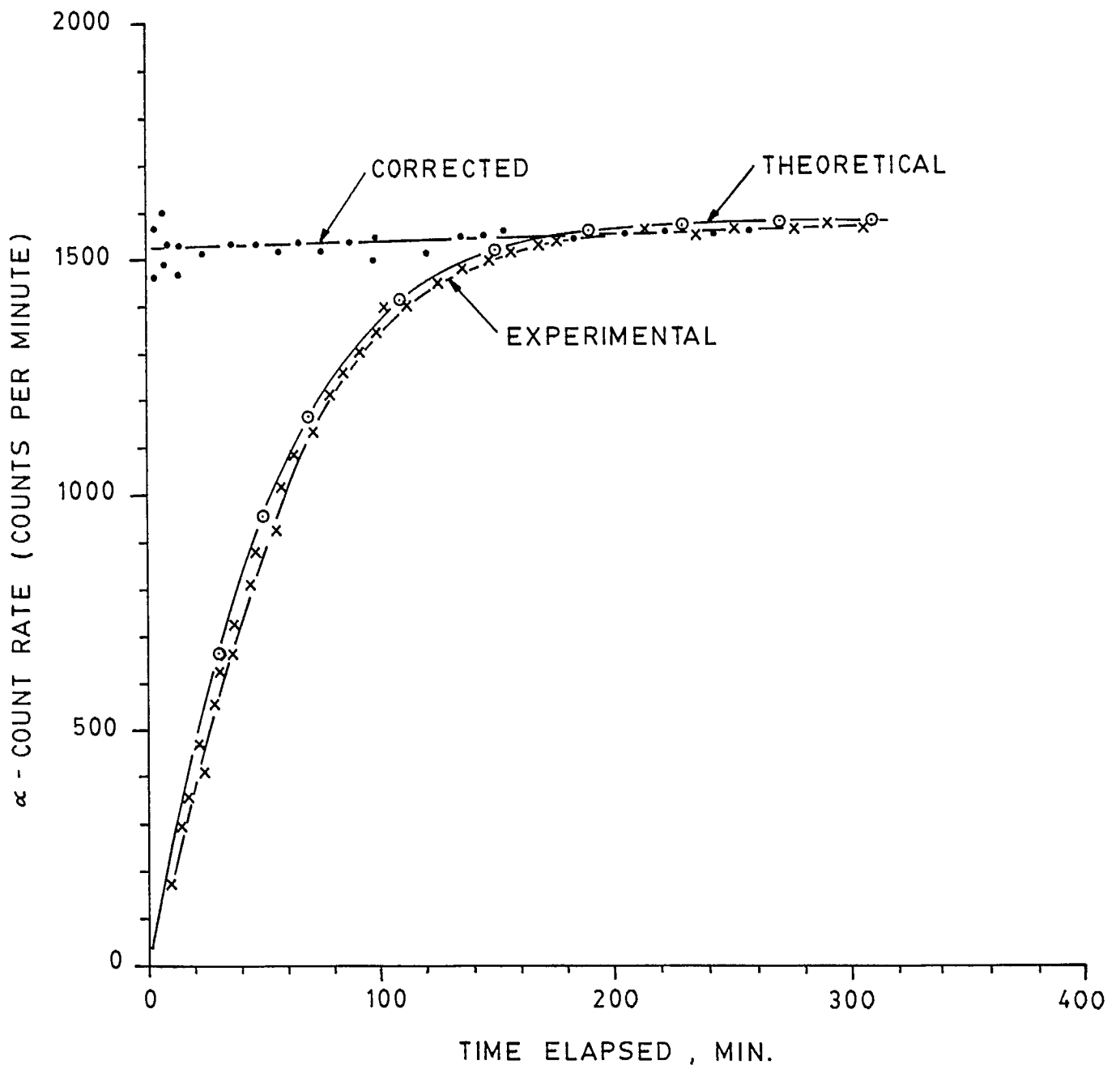


Figure 5

